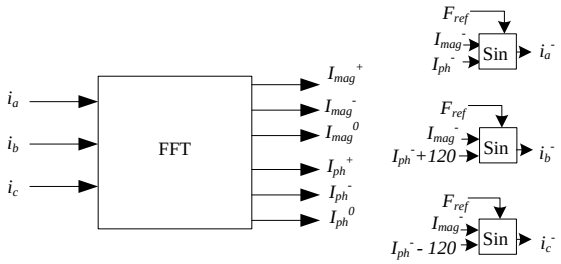


*Fig. 4 FFT based algorithm for unbalance extraction*

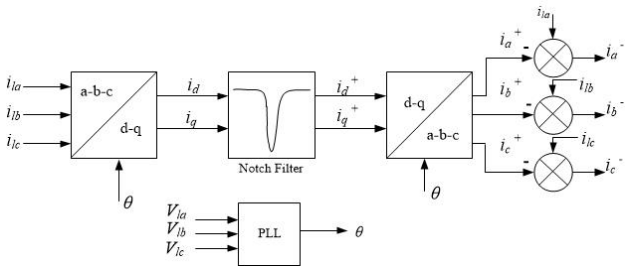


*Fig. 5 SRF-PLL Unbalance extraction theory*

## 4. Simulation results

The proposed control system for WECS to regulate tertiary winding voltage and unbalance mitigation is simulated on PSCAD/EMTDC program. Different case studies are conducted to evaluate the dynamic performance of the proposed WECS. Comparison of the ANF, the FFT and SRF methods used for unbalance mitigation are presented.

### *A. WECS performance and Voltage regulation*

Table 1 illustrates the WECS model parameters. As shown in Fig. 6, the wind velocity changes from 5 m/s to 13.4 m/s at *t*=6 s, while the generator power changes from 69.3 kW to 1260 kW once the rotational speed of the generator reaches the new optimal setting. The DC link reference voltage is tightly regulated at 1.3 kV as shown in Fig. 6(c). To keep DC link voltage, $i_d^*$ is changed from 0.23 kA to 1.63 kA as illustrated in Fig. 6(d). Fig. 7(a) and (b) shows the output active and reactive power from the WECS at the generator side and at the grid side. At the beginning, the wind speed is slow, so the output active power is low and extra power is needed to supply the load. As a result, the grid contributes with the WECS to supply the load. After *t*=6 s, when the wind speed increased to 13.4 m/s, due to inertia of the turbine the output power ramp up until it reaches nominal value at *t*=7.6 s. The output power from the WECS is high enough to supply the load, and the remaining power is transferred to the grid. Also, the reactive power provided by the WECS increases to compensate for the load voltage.

Table 1- System Parameters

| | |
|---|---|
| Tertiary transformer winding voltages (MV grid, wind turbine & local load) | 22, 0.7, 0.38 kV |
| PMSG voltage and power ratings | 0.7 kV, 1.3 MW |
| DC link voltage | 1.3 kV |
| Frequency | 50 Hz |

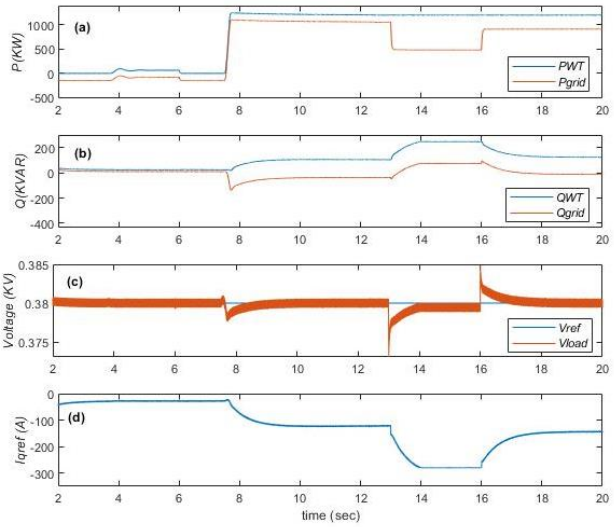


*Fig. 6 (a) Wind speed (b) Generator speed (c) DC link voltage (d) $i_d$* of the grid side converter.*

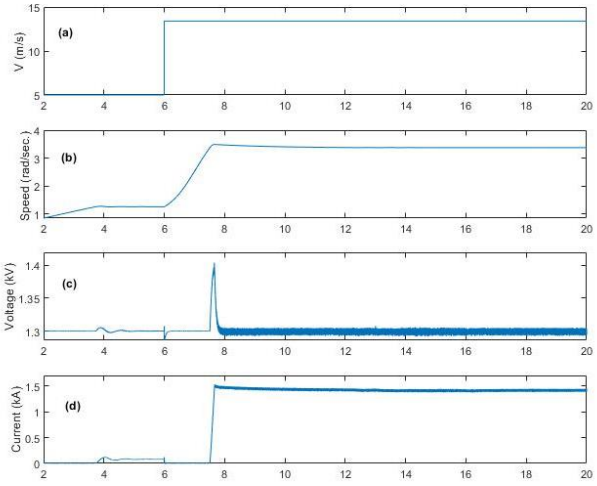


*Fig. 7 (a),(b) Active and reactive power at the WECS and grid sides, (c) load voltage, and (d) $i_q$* of the grid side converter.*

To examine the dynamic performance of the load voltage control loop, the load is increased at *t*=13 s, then is reduced to 50% at *t*=16 s. Fig. 7(c) demonstrates tight load voltage regulation by controlling $i_q^*$ as illustrated in Fig. 7(d). As expected, when the load increases, 13 s<*t*<16 s, the active power delivered to grid reduces. In addition, the reactive current of the grid-side converter increases to regulate the load. It can be noticed that $i_q^*$ is limited to a value such that the reactive power doesn't exceed 15 % of the active power supplied by the WECS. When the load is reduced at *t*=16 s, the load voltage rises and $i_q^*$ is decreased to keep the load voltage at the set value, 380 V.

### *B. Negative sequence extraction and Unbalance mitigation*

This section is dedicated to compare the dynamic performance of the ANF to extract the negative and positive sequence components with the FFT and the SRF methods. An unbalance load of 46% is connected to the system at *t*=8 s and the unbalance factor is reduced to 30%

at $t$ =15 s. Fig. 9(a) shows the negative sequence component of phase '*a*' obtained using the ANF, SRF, and FFT methods. It can be observed that the ANF converges faster than the SRF and FFT methods. The FFT is the slowest in response. The estimated positive sequence component is shown in Fig. 8(b) where the ANF also shows the fastest response in detecting the change in the sequence components at 8 sec. Fig. 9(a) and (b) demonstrate the estimated negative and positive sequence components during the transition from 46 % load unbalance to 30% load unbalance. It is clear, that the ANF extracts the symmetrical components smoothly and faster than the other methods. The results reveals that the dynamic performance of the ANF outdoes the conventional methods.

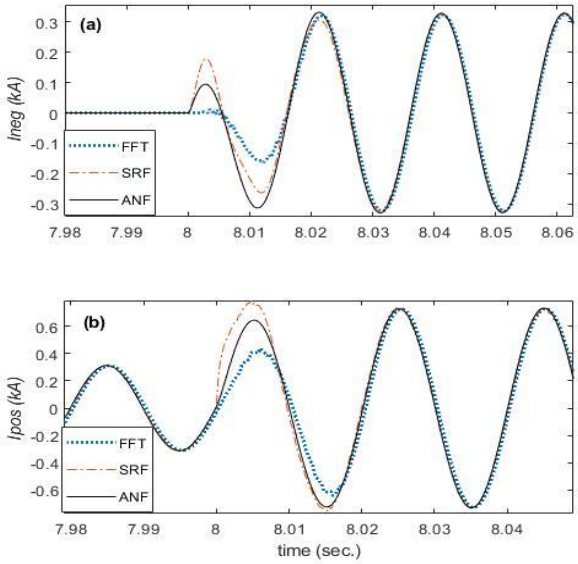


*Fig. 8 (a) Negative sequence component and (b) positive sequence component of phase a at 46% unbalance*

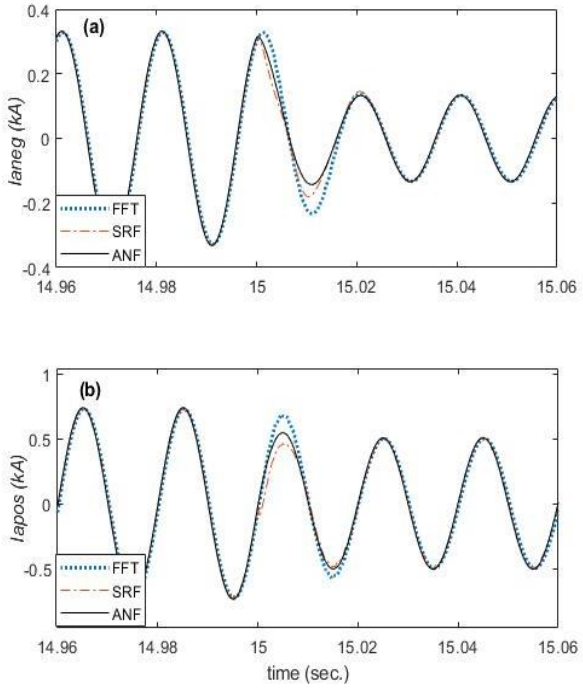


*Fig. 9(a) Negative sequence component and (b) positive sequence component of phase a at 30% unbalance*

The compensation for unbalance is enabled from $t$=10 s to $t$=17 s. Fig. 10(a) illustrates the grid currents at 46% load unbalance just before enabling the unbalance mitigation control loop and after enabling it at $t$=10 s. It is obvious that the proposed ANF succeeds to balance the grid current while the load current remains unchanged as demonstrated in Fig 10(b). Fig. 11(a) shows the grid currents at 30% load unbalance where the unbalance mitigation loop is disabled at at $t$=17 s to evaluate the dynamic performance of the system. As expected, the load current is not affected by the unbalance mitigation loop as shown in Fig.11(b).

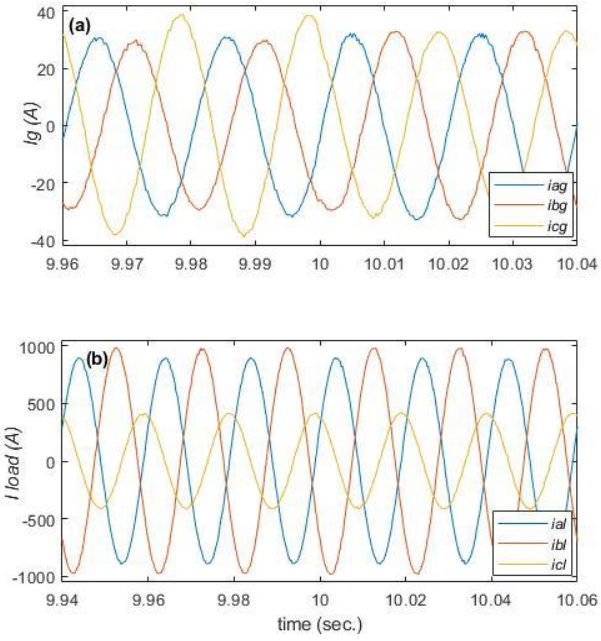


*Fig. 10 (a) three-phase grid currents at 46% unbalance (b) three-phase grid currents at 46% unbalance*

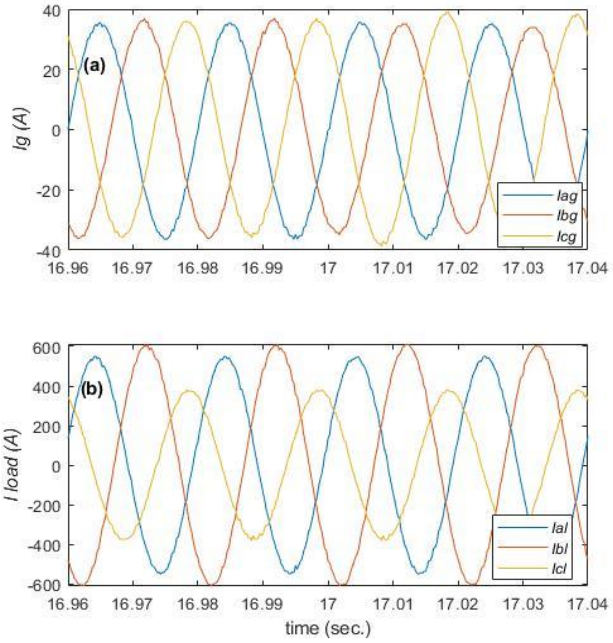


*Fig.11 (a) three-phase grid currents at 30% unbalance (b) three-phase grid currents at 30% unbalance*

## 5. Conclusion

This paper presents control loop for WECS to improve power quality level by regulating the voltage at the tertiary winding of the interfacing transformer and mitigating load unbalance. Voltage regulation of the local connected load is tested under different loading conditions and voltage level is maintained at its desired level. Unbalance mitigation is investigated using three different sequence components estimation methods. The ANF exhibits the best performance over the SRF and the FFT in convergence speed, adding to its unique feature of detecting the system frequency. The ANF is used in the control loop of unbalance mitigation and the grid current is accurately balanced at different load unbalance conditions.

### REFERENCES


[1] X. Tan, J. Dai, and B. Wu, "A novel converter configuration for wind applications using PWM CSI with diode rectifier and buck converter,"IEEE International Electr ic Machines & Drives Conference (2011), pp. 359-364

[2] M. I. Marei, A. Mohy, and A. A. El-Sattar "An Integrated Control System for Sparse Matrix Converter Interfacing PMSG with the Grid," International Journal of Electrical Power & Energy Systems (2015), Vol. 73, pp. 340-349.

[3] Rong Cai, M. Bongiorno and A. Sannino, "Control of D-STATCOM for voltage dip mitigation," International Conference on Future Power Systems (2005) pp. 6 pp.-6.

[4] M. Coppo, A. Raciti, R. Caldon and R. Turri, "Exploiting inverter-interfaced DG for Voltage unbalance mitigation and ancillary services in distribution systems," IEEE 1st International Forum on Research and Technologies for Society and Industry Leveraging a better tomorrow (2015),pp. 371-376.

[5] L. Xu, Z. Miao, L. Fan and G. Gurlaskie, "Unbalance and harmonic mitigation using battery inverters," 2015 North American Power Symposium (2015) pp. 1-6.

[6] M. I. Marei, T. El-Fouly, E. F. El-Saadany and M. M. A. Salama, "A Flexible Wind Energy Scheme for Voltage Compensation and Flicker Mitigation," IEEE Proceeding of General Meeting (2003), Toronto, Canada.

[7] M.I. Marei and H. El-Goharey, "Modeling and Dynamic Analysis of Gearless Variable-Speed Permanent Magnet Synchronous Generator Based Wind Energy Conversion System" Renewable Energy and Power Quality Journal (2012), Vol. 10, pp. 1597-1602.

[8] J. Burkard and J. Biela, "Evaluation of topologies and optimal design of a hybrid distribution transformer,"17th European Conference on Power Electronics and Applications(2015),pp.1-10.

[9] J. Burkard and J. Biela, "Transformer inrush current mitigation concept for hybrid transformers,"19th European Conference on Power Electronics and Applications (2017), pp. P.1-P.9.

[10] D. P. Balachandran, R. S. Kumar and V. P. Shimnamol, "Transformer Inrush Current Reduction by Power Frequency Low Voltage Signal Injection to the Tertiary Winding," IEEE Lausanne Power Tech (2007), pp. 1953-1958.

[11] A. Mishal Abd-Elrasool Elagab and I. Mohamad El-Amin, "Minimization of Harmonics Penetration into Transmission and Distribution Systems by Utilizing Tertiary Winding of the Transformer,"9th IEEE-GCC Conference and Exhibition (2017), pp. 1-9.

[12] B. C. Sujatha, T. V. Ramaswamy, R. R. Prabhu, N. Sumana, D. M. U and S. Z. Ismail, "Design of 100kVA energy efficient three phase hybrid transformer for combined application of solar and wind," 4th International Conference for Convergence in Technology (2018), pp. 1-4.

[13] M. I. Marei, E. F. El-Saadany and M. M. A. Salama, "An Intelligent Control for the DG Interface to Mitigate Voltage Flicker," 18th IEEE Applied Power Electronics Conference (2003), Florida, USA.

[14] M. I. Marei, "A unified control strategy based on phase angle estimation for matrix converter interface system," IEEE Systems Journal (2012), Vol. 6, No. 2, pp. 278-286.

[15] M. I. Marei, E. F. El-Saadany, and M. M. A. Salama, "Experimental evaluation of envelope tracking techniques for voltage disturbances," Electric Power Systems Research (2010), Vol. 80, No. 3, pp. 339 – 344.

[16] S. P. Gopal and D. R. Patil, "Hysteresis Band Current Controller for voltage regulation and harmonic mitigation using DSTATCOM," International Conference on Computation of Power, Energy Information and Commuincation Chennai (2016), pp. 707-712.

[17] M. I. Marei, E. F. El-Saadany and M. M. A. Salama, "A Novel Control Scheme for STATCOM Using Space Vector Modulation Based Hysteresis Current Controller," 11th International Conference on Harmonics and Quality of Power (2004), USA.

[18] A. R. Malekpour, A. Pahwa and S. Das, "Inverter-based var control in low voltage distribution systems with rooftop solar PV," North American Power Symposium (2013), Manhattan, KS, 2013, pp. 1-5.

[19] W. Lyu et al., "A Novel Three Phase Unbalance Detection and Compensation method of Active Power Filter," Chinese Automation Congress (2018), pp. 418-422.

[20] R. S. Herrera, P. SalmerÓn and H. Kim, "Instantaneous Reactive Power Theory Applied to Active Power Filter Compensation: Different Approaches, Assessment, and Experimental Results," in IEEE Transactions on Industrial Electronics (2008), vol. 55, no. 1, pp. 184-196.

[21] Anu P, Divya R and M. G. Nair, "STATCOM based controller for a three phase system feeding single phase loads," International Conference on Technological Advancements in Power and Energy (2015), pp. 333-338.

[22] Z. Wang, Y. Li and H. Zhang, "Harmonic Detection Method Based on Windowed Double-Spectrum Interpolation FFT," International Conference on Robots & Intelligent System (2019), pp. 425-427.

[23] M. Sun and Z. Sahinoglu, "Extended Kalman filter based grid synchronization in the presence of voltage unbalance for smart grid," ISGT (2011), Anaheim, CA, pp. 1-4.

[24] M. I. Marei, E. F. El-Saadany and M. M. A. Salama, "A processing unit for symmetrical components and harmonics estimation based on a new adaptive linear combiner structure," in IEEE Transactions on Power Delivery (2004), vol. 19, no. 3, pp. 1245-1252.

[25] L. S. Xavier, A. F. Cupertino, V. F. Mendes and H. A. Pereira, "Detection method for multi-harmonic current compensation applied in three-phase photovoltaic inverters," 12th IEEE International Conference on Industry Applications (2016), pp. 1-8.

[26] D. Yazdani, M. Mojiri, A. Bakhshai and G. JoÓs, "A Fast and Accurate Synchronization Technique for Extraction of Symmetrical Components," in IEEE Transactions on Power Electronics (2009), vol. 24, no. 3, pp. 674-684.

[27] A. A. Abu El-Naga, M. I. Marei, and H. S. K. El-Goharey, "Second Order Adaptive Notch Filter Based Wind Power Smoothing Using Flywheel Energy Storage System," 19th IEEE International Middle East Power Systems Conference (2017), pp. 314-319.